TRANSACTIONS ON EMERGING TELECOMMUNICATIONS TECHNOLOGIES
Trans. Emerging Tel. Tech. 2015; **26**:56–69
Published online 6 November 2014 in Wiley Online Library (wileyonlinelibrary.com). DOI: 10.1002/ett.2891

SPECIAL ISSUE PAPER

Duty cycle control with joint optimisation of delay and energy efficiency for capillary machine-to-machine networks in 5G communication system

Yun Li[1]*, Kok Keong Chai[1], Yue Chen[1] and Jonathan Loo[2]

[1] School of Electronic Engineering and Computer Science, Queen Mary University of London, London, E1 4NS, UK
[2] School of Science and Technology, Middlesex University, London NW4 4BT, UK

ABSTRACT

A hybrid network architecture has been proposed for machine-to-machine (M2M) communications in the fifth generation wireless systems, where M2M gateways connect the capillary networks and cellular networks. In this paper, we develop novel energy efficient and end-to-end delay duty cycle control scheme for controllers at the gateway and the capillary networks coordinator. We first formulate a duty cycle control problem with joint-optimisation of energy consumption and end-to-end delay. Then, a distributed duty cycle control scheme is proposed. The proposed scheme consists of two parts (i) a transmission policy, which decides the optimal number of packets to be transmitted between M2M devices, coordinators and gateways; and (ii) a duty cycle control for IEEE 802.15.4. We analytically derived the optimal duty cycle control and developed algorithms to compute the optimal duty cycle. It is to increase the feasibility of implementing the control on computation-limited devices where a suboptimal low complexity rollout algorithm-based duty cycle control (RADutyCon) is proposed. The simulation results show that RADutyCon achieves an exponential reduction of the computation complexity as compared with that of the optimal duty cycle control. The simulation results show that RADutyCon performs close to the optimal control, and it performs no worse than the heuristic base control. Copyright © 2014 John Wiley & Sons, Ltd.

***Correspondence**
Yun Li, School of Electronic Engineering and Computer Science Queen Mary University of London, London, E1 4NS, UK.
E-mail: yun.li@qmul.ac.uk

Received 20 June 2014; Accepted 14 September 2014

1. INTRODUCTION

Machine to machine (M2M) networks represents a future Internet of Things (IoT) which is expected to be widely utilised in many fields, including smart cities, smart grids, industrial and agricultural automations, health care and transport systems [1–7]. As the traditional voice service revenues continue to shrink, the mobile network operators are increasingly interested in M2M applications to bridge in the growing revenue gap [8]. In addition, M2M communication has been listed one of the horizontal topics of the Europe METIS 2020 project [9]. More recently, following the study of M2M support in LTE-Advanced networks [10–14], M2M communication has been identified as one of the key drivers to guide the design of 5G network [15, 16]. The goal of Fifth Generation (5G) system is to accommodate the challenges of continuously increasing demand for higher data rates, larger network capacity, higher spectral efficiency, higher energy efficiency, and higher mobility required by new wireless applications [17]. Thus, enabling M2M communication in 5G communication system has become the next big opportunity and challenge for both industry operators and academia researchers.

Mobile stakeholders and standardisation organisations have identified the need for supporting M2M applications through cellular networks [18]. The major benefit of supporting M2M applications in cellular networks is the ubiquitous wireless access in both urban and rural environments on the existing wireless cellular infrastructure, which means there is no need to build alternate infrastructures. However, the low mobility, stringent cost and energy efficiency requirements of M2M devices make the design criteria of M2M communication very different from that of cellular networks. The challenges of direct connecting M2M devices with cellular networks including the following:

(i) Cost: The overall device cost will be high as all M2M devices need to equip a cellular interface to connect with the cellular base station.
(ii) Quality of Service (QoS): The heavy contention will lead to serious QoS problems when there are huge amount of simultaneous connections.
(iii) Small data packet transmission: The cellular networks are designed for supporting broadband applications, which traditionally transmit large number of packet, whilst most M2M applications only transmit small amounts of data with low data rates. This leads to low channel utility and unreasonable ratio between payload and required control information.
(iv) Energy consumption: The need to provide direct cellular access may lead to excessive energy consumption, which is a major problem for battery-powered devices.

To address the aforementioned challenges, European Telecommunication Standards Institute M2M Technical Committee has proposed an attempt to support M2M communication in 5G systems with a hybrid architecture [19]. Instead of direct cellular access, a large number of non-cellular M2M devices using short-range, low-cost, low-energy consumption radio interfaces, such as IEEE 802.15.4 or IEEE 802.11 to connect to the base station via M2M gateways. The network of the non-cellular M2M devices are called capillary networks [20]. The M2M gateways act as traffic aggregation and protocol translation points for their capillary networks to LTE networks [21]. In this way, the capillary M2M networks ensure the low cost per terminal, low energy consumption, shaping the traffic by off-loading and grouping M2M devices into smaller numbers [22]. Recently, a European founded project, EXpAnding LTE for Devices (EXALTED) [23] also proposed a similar solution to M2M communication. In EXALTED, M2M communications between capillary networks is supported by a new LTE-M backbone, which will be a 3GPP Release 8 compatible extension of LTE network. Besides the efforts of standard organisations and academia researches, there are also a large number of industry projects, such as [24–29], try to exploit such hybrid architecture with actual commercial products and solutions.

As the massive access of M2M devices in the capillary networks to LTE networks is ensured via M2M gateways, novel access control algorithms for the M2M gateways and coordinators of capillary networks are necessary to ensure the performance of network throughput, delay and energy efficiency. In this paper, we will focus on the control at M2M gateways and coordinators of capillary network. We focus on IEEE 802.15.4-2011 [30] as the capillary networks interface, because it is one of the most promising short-range technologies to implement on the capillary portion of the M2M architecture [31, 32].

IEEE 802.15.4-2011 standard utilises a duty cycle-based medium access control (MAC) protocol to achieve the energy efficiency; however, it introduces some challenges for IEEE 802.15.4-2011 to support capillary M2M communication in 5G communication system. First, the energy efficiency of IEEE 802.15.4-2011 is achieved by applying duty cycle, which periodically puts the device into sleep. However, a lower duty cycle will introduce sleep delay as the sender may have to wait until the receiver becomes active [33]. In multi-hop network, this will highly degrade the end-to-end delay performance as the sleep delay will cumulate hop by hop. Second, the centralised uniformed duty cycles for all devices in current standard may not provide the best overall performance to meet the various requirements of applications and different device capabilities. Thus, a flexible distributed duty cycle control, which can meet various QoS requirement of different M2M devices, is highly desired.

The contributions of the paper are summarised as follows:

(i) A duty cycle control problem is formulated to minimise the joint-cost of energy consumption and end-to-end delay in hybrid M2M networks. The diversity of both application requirements and M2M device capacities is taken into consideration.
(ii) A novel duty cycle control scheme is proposed to solve the duty cycle control problem. The control scheme is applicable for both M2M gateways and coordinators of capillary networks.
(iii) An optimal transmission policy and duty cycle control for IEEE 802.15.4 MAC layer is mathematical derived by applying dynamic programming (DP).
(iv) Two duty cycle control algorithms are proposed to compute the optimal duty cycle.
(v) A new low complexity rollout algorithm-based duty cycle control (RADutyCon) is proposed to further reduce the computational complexity.

The remainder of the paper is organised as follows. In Section 2, we give some background about existing work on duty cycle control with joint consideration of energy efficiency and end-to-end delay. The system model and background of IEEE 802.15.4-2011 MAC protocol are introduced in Section 3. The problem formulation is given in Section 4. In Section 5, by applying dynamic programming, the optimal duty cycle control is derived, followed by two algorithms to compute the optimal duty cycle control for IEEE 802.15.4-based capillary networks. To strike a reasonable balance between computational complexity and performance for battery-powered M2M devices, a suboptimal low complexity RADutyCon is proposed in Section 6. In the end, simulation results and conclusion are given in Sections 7 and 8, respectively.

2. RELATED WORK

There are some existing work that focus on duty cycle control with the aim of reducing the delay and energy consumption. Traffic Aware Scheduling Algorithm (TASA) is

proposed in [34], which focus on building time/frequency patterns based on the network topology and the traffic load at each node. TASA aims at minimising the number of active slots, necessary for delivering to the PAN coordinator the traffic load, offered to the network. However, the centralised control of TASA may limit its scalability when applying into capillary M2M networks. In [35], DutyCon is proposed to guarantee end-to-end delay by assigning a local delay requirement to each single hop along the communication flow. In this method, a feedback controller is designed to adapt the sleep interval to meet the single-hop delay requirement. However, this approach requires significant amount of signalling from the neighbour devices to compute the delay. To reduce the signalling amongst neighbour devices, a distributed duty cycle controller is proposed in [36] aiming at controlling the local queue length of the device to be the same as the predetermined threshold. The distributed duty cycle control is achieved by adjusting the sleep duration of each device based on its local queue length independently. However, this approach needs specific syntonisation scheme, and the evolution of the proposed control requires carefully setting of the initial duty cycle and control parameters. More recently, an adaptive optimal duty-cycle algorithm running on top of IEEE 802.15.4 MAC protocol is proposed in [37]. Adaptive optimal duty-cycle algorithm aims at minimising energy consumption whilst meeting the reliability and delay requirements. However, this work focuses on the non-beacon-enabled mode of IEEE 802.15.4.

Our previous work [38] proposed a RADutyCon for IEEE 802.15.4-based networks. The aim of [38] is to achieve a joint optimisation of energy consumption and end-to-end delay by controlling the duty cycle for IEEE 802.15.4-based networks. In this paper, we extend our previous work to support capillary M2M communication in 5G communication system. A distributed duty cycle control scheme is proposed for the controllers at the gateway and the coordinator in capillary M2M networks. The proposed scheme consists of two parts: (i) a transmission policy, which decides the optimal number of packets to be transmitted between M2M devices, coordinators and gateways; and (ii) a duty cycle control for IEEE 802.15.4. In addition, by adjusting the duty cycle setting in second part accordingly, the proposed duty cycle control scheme can be extended to other technology interfaces provided by gateways, such as WiFi and Bluetooth. Special considerations have been taken into account in terms of low end-to-end delay, energy efficiency diverse device capabilities and various QoS requirements for capillary M2M in 5G communication system. It is worth to point out that, besides IEEE 802.15.4, our proposed scheme can also be extended to other duty cycle-based MAC protocols by adjusting the second part of the scheme accordingly.

3. SYSTEM MODEL

As described earlier, we focus on the capillary part of the M2M network in this paper. The system model of our work is shown in Figure 1. Amongst different multi-hop network topologies, a simple two-hop cluster-tree network model between gateway and M2M devices has been the focus of much ongoing research, as the multi-hop case can be viewed as the combination of several two-hop scenarios. M2M devices are connected in one of the clustered capillary networks, which is ultimately connected to the cellular base station through an M2M gateway.

There are N control devices (i.e. gateways and coordinators) in the network and M end M2M devices. The gateway/coordinator is denoted as n_i, whilst the M2M device is denoted as m_i. The level of the device is denoted as l_{n_i}. Thus, the cellular base station n_0 is in level-1, thus $l_{n_0} = 1$. The gateways and coordinators are in level-2 and level-3, respectively. The end M2M devices are in level-4. We denote the child M2M devices set of control device n_i as ch_{n_i}.

3.1. Queue and traffic models

We assume that all generated packets are available at the beginning of each period k (one active period and one inactive period). All the packets are forwarded to the cellular base station n_0 for uplink transmission and $q_{n_i}^{\max}$ is the maximum queue length of the device n_i. The new arrived packets will be dropped if the queue length in the buffer reaches its maximum $q_{n_i}^{\max}$. Similar to [36], the queue length change of device n_i is given as

$$q_{n_i}^{k+1} = \min\left(\left[q_{n_i}^{k} + r_{n_i}^{k} - f_{n_i}^{k} + g_{n_i}^{k}\right]^{+}, q_{n_i}^{\max}\right) \quad (1)$$

where $0 \leqslant k \leqslant K-1, [\cdot]^{+} = \max(0,\cdot), g_{n_i}^{k}$ is the number of packets being generated by device n_i in period k; $f_{n_i}^{k}$ is the number of packet transmitted by device n_i in period k; and $r_{n_i}^{k}$ is the number of packets received by device n_i in period k. Note that $r_{n_i}^{k}$ equals to zero if device n_i has no child device.

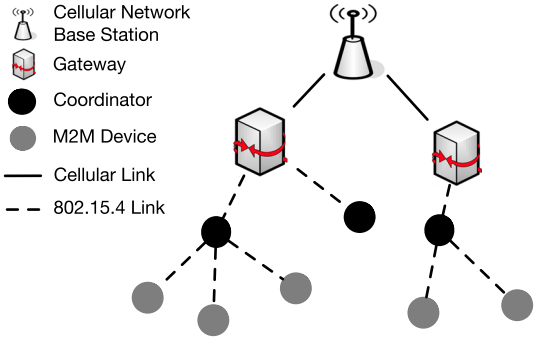

Figure 1. Network model.

Trans. Emerging Tel. Tech. **26**:56–69 (2015) © 2014 John Wiley & Sons, Ltd.
DOI: 10.1002/ett

Note that Poisson arrivals have been recently proposed for 3GPP machine-type communication traffic modelling regarding triggered M2M communications [39]. Thus, we assume that the number of packets each device sends to its parent device follows Poisson distribution and each device generates a Poisson distributed integer number of packets in each period, which means $f_{n_i}^k$ and $g_{n_i}^k$ are independent random variables.

3.2. Channel model

The channel propagation loss between devices is composed of losses due to distance, fading and shadowing. Based on [40], we assume a dual-slope model of path loss with distance, Nakagami frequency-flat small-scale fading and lognormal shadowing. The overall channel propagation loss is expressed as

$$L_{c,dB} = L_{0,dB} + X_{s,dB} + X_{f,dB} + \begin{cases} 10n_0 \log(d) & d \leqslant d_1 \\ 10n_0 \log(d_1) + 10n_1 \log\left(\frac{d}{d_1}\right) & d > d_1 \end{cases} \quad (2)$$

where d is the distance between the sender and receiver, $X_{f,dB} = 10\log(X_f)$ and X_f is a unit-mean gamma-distributed random variable with variance $1/m$ (where m is the Nakagami fading parameter); X_s dB is a zero mean Gaussian random variable with standard deviation σ_s, and all logarithms are base 10. We assume that the fading and shadowing are constant during each period.

The condition for the successful transmission is that the received signal power is above the sensitivity threshold $P_{sens,n_i}^k(dBm)$ of the device. The received power P_{rec,n_i}^k of device n_i is a function of the transmitted power, antenna gains and channel attenuation. It is modelled (in decibels referenced to 1 mw) as

$$P_{rec,n_i}^k = P_{tran,n_i}^k + G_{tran,n_i}^k + G_{rec,n_i}^k - L_{c,m_i}^k \quad (3)$$

where $m_i \in ch_{n_i}, P_{tran,n_i}^k(dBm)$ is the conducted power to the transmit antenna (dBm), $G_{tran,n_i}^k(dBi)$ and $G_{rec,n_i}^k(dBi)$ are the transmit and receive antenna gains (dBi), respectively, and L_{c,n_i}^k is the loss due to channel propagation. We denote the successful transmission probability of device n_i at period k as

$$\rho_{n_i,m_i}^k = \begin{cases} 1 & P_{rec,n_i}^k < P_{sens,n_i}^k \\ 0 & P_{rec,n_i}^k \geqslant P_{sens,n_i}^k \end{cases} \quad (4)$$

3.3. IEEE 802.15.4-2011

We adopt IEEE 802.15.4 (2011) beacon enabled, where beacon is transmitted to synchronise the network. The superframe structure of IEEE 802.15.4 MAC layer is shown in Figure 2. The duration between two consecutive beacons is called beacon interval (BI), whilst the duration of an active period is called superframe duration (SD).

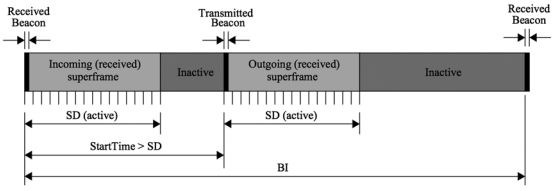

Figure 2. Superframe structure of IEEE 802.15.4 - 2011.

Specifically,

$$BI = aBaseSuperFrameDuration \times 2^{BO} \quad (5)$$

$$SD = aBaseSuperFrameDuration \times 2^{SO} \quad (6)$$

where beacon order (BO) and superframe order (SO) are two integers ranging from 0 to 14 ($0 \leqslant SO \leqslant BO \leqslant 14$), and $aBaseSuperFrameDuration = 15.36\ ms$ at 2.4 GHz with 250 kbps bandwidth. The duty cycle is defined as the ratio of the active portion over each period, thus

$$Duty\ cycle = SD/BI = 2^{SO-BO} \quad (7)$$

To achieve energy efficiency on for each coordinator, which is not the PAN coordinator by enabling duty cycling, IEEE 802.15.4-2011 defines incoming superframe in which the coordinator receives the beacon from its parents node and the outgoing superframe in which it transmits its own beacon to its child devices.

4. PROBLEM FORMULATION

In this section, the duty cycle control problem at gateway or coordinators of capillary networks is formulated with two parts: (i) an optimal transmission policy, which manages the number of received number of packets with the joint consideration of energy consumption and end-to-end delay and (ii) the duty cycle setting based on the optimal transmission policy. By adjusting the duty cycle setting in second part accordingly, the proposed duty cycle control scheme can be extended to other technology interfaces provided by gateways, such as WiFi and Bluetooth.

The proposed duty cycle control scheme is applicable for controller at gateways and coordinators in capillary M2M networks. Taking into account the local traffic, the position of the devices and types of applications, the controller can adapt the control parameters of the proposed duty cycle control scheme. More specifically, the hardware control parameters including: energy cost coefficients for receiving, transmitting, idle listening and delay cost coefficient. The application control parameters are the weighting factors on energy efficiency and end-to-end delay.

4.1. Transmission policy

The challenge of joint optimisation of energy efficiency and end-to-end delay is that they have different units.

Thus, it is difficult to combine these two terms in one objective function. To address this challenge, we need to find out a uniformed way to measure the energy efficiency and end-to-end delay. Luckily, packet transmission analysis provides a nature angle to measure the network performance with respect to the number of packets.

To this end, we define the transmitting energy consumption cost $E_t\left(f_{n_i}^k\right)$, receiving energy consumption cost $E_r\left(r_{n_i}^k\right)$, idle listening energy consumption cost $E_l\left(r_{n_i}^k\right)$ and end-to-end delay cost $D\left(r_{n_i}^k\right)$ of device n_i all in terms of packet numbers. The specific definition are given as

$$E_r\left(r_{n_i}^k\right) = c_r \times \frac{r_{n_i}^k}{q_{n_i}^{\max} \times l_{n_i}} \tag{8}$$

$$E_t\left(f_{n_i}^k\right) = c_f \times \frac{f_{n_i}^k}{q_{n_i}^{\max} \times l_{n_i}} \tag{9}$$

$$E_l\left(r_{n_i}^k\right) = c_l \times \frac{\left[f_{n_i}^k - g_{n_i}^k - q_{n_i}^k - r_{n_i}^k\right]^+}{q_{n_i}^{\max} \times l_{n_i}} \tag{10}$$

$$D\left(r_{n_i}^k\right) = c_d \times \frac{\left[q_{n_i}^k + r_{n_i}^k + g_{n_i}^k - f_{n_i}^k\right]^+}{q_{n_i}^{\max} \times l_{n_i}} \tag{11}$$

where $c_f \in (0,1), c_r \in (0,1), c_l \in (0,1)$ and $c_d \in (0,1)$ are the coefficients of transmitting, receiving, idle listening and delay of the device, respectively. Note that $c_r < c_l$, as if c_r were greater than c_l, it would never be optimal to receive new packets in the last period and possibly in earlier periods.

We further introduce α and β to assign the weightings of energy efficiency and end-to-end delay requirements of different applications. The expected weighted-sum joint-cost function for device n_i at period k is

$$\begin{aligned} J\left(r_{n_i}^k\right) = \mathbb{E}\Big\{\alpha\left(E_f\left(f_{n_i}^k\right) + E_r\left(r_{n_i}^k\right) + E_l\left(r_{n_i}^k\right)\right) \\ +\beta D\left(r_{n_i}^k\right)\Big\} \end{aligned} \tag{12}$$

Our objective is to find the control of the optimal duty cycles $\pi_{n_i}^*$ for each device n_i over K periods, which minimise the overall expected joint-cost. Hence, the joint optimisation problem is

$$\begin{aligned} \mathcal{P}_{n_i}: \quad \min_{\pi_{n_i} \in \mathfrak{D}} \quad & \mathbb{E}\left\{\sum_{k=0}^{K-1} \rho_{n_i,m_i}^k J\left(r_{n_i}^k\right)\right\} \\ \text{s.t.} \quad & m_i \in ch_{n_i} \\ & q_{n_i}^K = 0, \\ & r_{n_i}^k \leqslant r_{n_i}^{\max} \end{aligned} \tag{13}$$

where $\mathfrak{D}$ is valid duty cycle sets of device n_i and $r_{n_i}^{\max}$ is the maximum number of packets device n_i could receive. According to (1)–(3), the range of $\mathfrak{D}$ is restricted by the maximum valid *SO*.

4.2. Duty cycle control

IEEE 802.15.4 -2011 adopt slotted carrier-sense multiple access with slotted collision avoidance for packet transmission. Before the packet transmission, we assume devices need to perform two clear channel accesses (CCAs). Within each superframe duration, the beacon transmission duration is D_{bcn}. Thus, the total packet transmission duration

$$PD = SD - D_{bcn} = r_{n_i} \times P_s \tag{14}$$

If acknowledgement (ACK) is required for each packet, the successful packet transmission period

$$P_s = \lceil P_{CCA} + P_L + \delta + P_{ACK} \rceil \tag{15}$$

where P_{CCA} is the transmission time for two CCAs, P_L is the transmission time for each packet, δ and P_{ACK} are waiting and transmission time of the ACK packet, respectively.

Our duty cycle control is applicable in a distributed manner, in that each coordinator and gateway will decide its own incoming duty cycle based on its local traffic, whilst the outgoing superframe duty cycle is decided by its parent device and enclosed in the received beacon. To simplify the problem, all devices to be activated at the beginning of each *BI*. The same *BO* is set to all devices in the network with the aim of simplifying the synchronisation. Thus, the duty cycle control of each coordinator and gateway is achieved by setting the outgoing *SO* based on the number of packets generated by its child devices.

Because of the collision, the transmission throughput is limited according to the number of contending devices. We adopt the throughput limitation coefficient b of [41]. Based on (2), the relationship between *SO* and the amount of packets the device could receive in period k is given as follow

$$SO_{n_i}(k) = \left\lceil \log_2\left(\frac{r_{n_i}^k \times P_s}{b} + D_{bcn}\right)\right\rceil \tag{16}$$

5. OPTIMAL DUTY CYCLE CONTROL FOR IEEE 802.15.4

In this section, we first derive the optimal transmission policy of our problem and provide its proof. Then we give an online optimal duty cycle control for the gateways and coordinators in the capillary networks.

Trans. Emerging Tel. Tech. **26**:56–69 (2015)
DOI: 10.1002/ett

5.1. Optimal transmission policy

We solve the problem $\mathcal{P}_{n_i}$ by applying the principle of DP [42]. For each capillary M2M network with gateway n_i, the outage probability $\rho^k_{n_i,m_i}$ is measured according to (2)–(4). For all devices m_i with $\rho^k_{n_i,m_i} = 1$, the $\mathcal{P}_{n_i}$ can be decomposed into a sequence of subproblems $\mathcal{S}\left(r^k_{n_i}\right)$, where$k \in (0, K)$. The cost-to-go function $U\left(r^k_{n_i}\right)$, which is the sum of joint-cost functions from period k to K is given as

$$U\left(r^k_{n_i}\right) = \min_{\pi_{n_i}\in\mathfrak{D}} \mathbb{E}\left\{\alpha\left(E_r\left(r^k_{n_i}\right) + E_t\left(f^k_{n_i}\right)\right) + H\left(r^k_{n_i}\right) + \mathbb{E}\left\{U\left(r^{k+1}_{n_i}\right)\right\}\right\} \tag{17}$$

where

$$H\left(r^k_{n_i}\right) = \mathbb{E}\left\{\alpha E_l\left(r^k_{n_i}\right) + \beta D\left(r^k_{n_i}\right)\right\} \tag{18}$$

shows the tradeoff between idle listening energy consumption cost and the end-to-end delay cost.

The objective of each subproblem $\mathcal{S}\left(r^k_{n_i}\right)$ is to minimise the cost-to-go function $U\left(r^k_{n_i}\right)$ from period k to K

$$\mathcal{S}\left(r^k_{n_i}\right): \quad \min_{\pi_{n_i}\in\mathfrak{D}} \quad \mathbb{E}\left\{\sum_{k=0}^{K-1} U\left(r^k_{n_i}\right)\right\} \quad \text{s.t.} \quad q^K_{n_i} = 0, \quad r^k_{n_i} \leqslant r^{\max}_{n_i} \tag{19}$$

To solve the subproblem $S\left(r^k_{n_i}\right)$, we introduce $m^k_{n_i} = q^k_{n_i} + r^k_{n_i}$ and $n^k_{n_i} = f^k_{n_i} - g^k_{n_i}$ for simplicity. Then, combined with (10) and (11), $H\left(r^k_{n_i}\right)$ in (18) can be rewritten as

$$H\left(m^k_{n_i}\right) = \mathbb{E}\left\{\alpha c_l \times \frac{\max\left(q^{\max}_{n_i}, \left[n^k_{n_i} - m^k_{n_i}\right]^+\right)}{q_{\max} \times l_{n_i}} + \beta c_d \times \frac{\max\left(q^{\max}_{n_i}, \left[m^k_{n_i} - n^k_{n_i}\right]^+\right)}{q_{\max} \times l_{n_i}}\right\} \tag{20}$$

As the convexity preserved by taking expectation over $n^k_{n_i}$, with each fixed $n^k_{n_i}, H\left(m^k_{n_i}\right)$ is convex. Because of the convexity of $H\left(m^k_{n_i}\right)$, we rewrite (17) as

$$U\left(m^k_{n_i}\right) = \min_{\pi_{n_i}\in\mathfrak{D}} \mathbb{E}\left\{W\left(m^k_{n_i}\right) - \alpha c_r \times \frac{q^k_{n_i}}{q_{\max} \times l_{n_i}}\right\} \tag{21}$$

where

$$W\left(m^k_{n_i}\right) = \alpha c_r \times m^k_{n_i} + \alpha \times E_f\left(f^k_{n_i}\right) + H_{n_i}\left(m^k_{n_i}\right) + \mathbb{E}\left\{U\left(m^{k+1}_{n_i}\right)\right\} \tag{22}$$

Then the objective of each subproblem $\mathcal{S}\left(r^k_{n_i}\right)$ is to find the minimum value of (21).

Before we give the solution to each subproblem $\mathcal{S}\left(r^k_{n_i}\right)$, we present a sufficient condition for the convexity of functions $W\left(m^k_{n_i}\right)$ in Lemma 1:

Lemma 1. *If $H\left(m^k_{n_i}\right)$ and $U\left(m^k_{n_i}\right)$ are convex functions, so is $W\left(m^k_{n_i}\right)$.*

Proof. Based on the definition of convex function, $W\left(m^k_{n_i}\right)$ is convex if

$$W\left(\frac{m^k_{n_i} + \bar{m}^k_{n_i}}{2}\right) \leqslant \frac{W\left(m^k_{n_i}\right) + W\left(\bar{m}^k_{n_i}\right)}{2} \tag{23}$$

After eliminating, it is clear that (23) is satisfied if (24) follows. Because $H\left(m^k_{n_i}\right)$ and $U\left(m^k_{n_i}\right)$ are convex functions, we have

$$H\left(\frac{m^k_{n_i} + \bar{m}^k_{n_i}}{2}\right) + \mathbb{E}\left\{U\left(\frac{\left(m^k_{n_i}+1\right) + \left(\bar{m}^k_{n_i}+1\right)}{2}\right)\right\} \leqslant \frac{H\left(m^k_{n_i}\right) + H\left(\bar{m}^k_{n_i}\right)}{2} + \frac{\mathbb{E}\left\{U\left(m^k_{n_i}+1\right) + U\left(\bar{m}^k_{n_i}+1\right)\right\}}{2} \tag{24}$$

$$H\left(\frac{m^k_{n_i} + \bar{m}^k_{n_i}}{2}\right) \leqslant \frac{H\left(m^k_{n_i}\right) + H\left(\bar{m}^k_{n_i}\right)}{2} \tag{25}$$

and

$$U\left(\frac{\left(m^k_{n_i}+1\right) + \left(\bar{m}^k_{n_i}+1\right)}{2}\right) \leqslant \frac{U\left(m^k_{n_i}+1\right) + U\left(\bar{m}^k_{n_i}+1\right)}{2} \tag{26}$$

Adding (25) and (26), the inequality (23) is satisfied. Thus, $W\left(m^k_{n_i}\right)$ is also a convex function.

Based on Lemma 1, the following theorem gives the optimal transmission policy of problem $\mathcal{P}_{n_i}$.

Theorem 1. *If $W\left(m^k_{n_i}\right)$ is convex, and the minimising scalars of $W\left(m^k_{n_i}\right)$ denoted as*

$$m^{k*}_{n_i} = T_{n_i} = \arg\min_{m^k_{n_i}\in\Re} W\left(m^k_{n_i}\right) \tag{27}$$

where $\Re$ is the set of all valid values of $m^k_{n_i}$.

Based on (27) and taking $r^k_{n_i} = m_{n_i} - q^k_{n_i}$, the minimum cost-to-go function value is attained at $r^k_{n_i} = T_{n_i} - q^k_{n_i}$ if

$q_{n_i}^k < T_{n_i}$, *and at* $r_{n_i}^k = 0$, *otherwise. Thus, the optimal transition policy of* $\mathcal{P}_{n_i}$ *is*

$$r_{n_i}^{k*} = \begin{cases} T_{n_i} - q_{n_i}^k & \text{if} \quad q_{n_i}^k < T_{n_i}, \\ 0 & \text{if} \quad q_{n_i}^k \geqslant T_{n_i}. \end{cases} \tag{28}$$

Proof. Based on Lemma 1 and (17)–(22), the convexity of $W\left(m_{n_i}^k\right)$ can be proved if the functions $U\left(m_{n_i}^k\right)$ are convex functions, and $\lim_{\left|m_{n_i}^k\right|} W\left(m_{n_i}^k\right) = \infty$.

For $k = K$, function $U\left(m_{n_i}^K\right)$ is a zero function, so it is convex.

$$r_{n_i}^{K-1} = \begin{cases} T_{n_i} - q_{n_i}^{K-1} & \text{if} \quad q_{n_i}^k < T_{n_i}, \\ 0 & \text{if} \quad q_{n_i}^k \geqslant T_{n_i} \end{cases} \tag{29}$$

$$U\left(r_{n_i}^{K-1}\right) = \begin{cases} \alpha \cdot c_r\left(T_{n_i} - q_{n_i}^{K-1}\right) + \alpha \cdot E_f\left(f_{n_i}^{K-1}\right) + H\left(r_{n_i}^{K-1}\right) & \text{if} \quad q_{n_i}^k < T_{n_i}, \\ \alpha \cdot E_f\left(f_{n_i}^{K-1}\right) + H\left(r_{n_i}^{K-1}\right) & \text{if} \quad q_{n_i}^k \geqslant T_{n_i} \end{cases} \tag{30}$$

$$U\left(r_{n_i}^k\right) = \begin{cases} \alpha \cdot c_r\left(T_{n_i} - q_{n_i}^k\right) + \alpha \cdot E_f\left(f_{n_i}^{k-1}\right) + H\left(r_{n_i}^k\right) + \mathbb{E}\left\{U\left(r_{n_i}^{k+1}\right)\right\} & \text{if} \quad q_{n_i}^k < T_{n_i}, \\ \alpha \cdot E_f\left(f_{n_i}^{k-1}\right) + H\left(r_{n_i}^k\right) + \mathbb{E}\{U(k+1)\} & \text{if} \quad q_{n_i}^k \geqslant T_{n_i} \end{cases} \tag{31}$$

As $c_r < c_l$, and the derivative of $H\left(m_{n_i}^K\right)$ tends to $-c_l$ as $m_{n_i}^k \to -\infty$. Thus, $H\left(m_{n_i}^K\right)$ is convex. Based on Lemma 1, given the convexity of $U\left(m_{n_i}^K\right)$, $W\left(m_{n_i}^K\right)$ is also convex. In addition, $W\left(m_{n_i}^K\right)$ has a derivative that becomes negative as $m_{n_i}^K \to -\infty$ and becomes positive as $m_{n_i}^K \to \infty$, thus

$$\lim_{\left|m_{n_i}^K\right| \to \infty} W\left(m_{n_i}^K\right) = \infty$$

Because $W\left(m_{n_i}^{K-1}\right)$ is minimised by T_{n_i}, the convexity of $U\left(m_{n_i}^{K-1}\right)$ is obvious. Furthermore, we have

$$\lim_{\left|m_{n_i}^{K-1}\right| \to \infty} U\left(m_{n_i}^{K-1}\right) = \infty$$

As shown earlier, the optimal policy at time $K-1$ is given by (29). The cost-to-go function at the period $K-1$ is derived as (30).

For $k = K-1, \cdots, 0$, the aforementioned arguments can be repeated: if $U\left(m_{n_i}^{k+1}\right)$ is convex; $\lim_{|m_{n_i}| \to \infty} U\left(m_{n_i}^k\right) = \infty$; and $\lim_{|m_{n_i}| \to \infty} W\left(m_{n_i}^k\right) = \infty$.

Recursively, the cost-to-go functions can be derived as (31), and $U\left(m_{n_i}^k\right)$ is convex; $\lim_{\left|m_{n_i}^{k-1}\right| \to \infty} U\left(m_{n_i}^{k-1}\right) = \infty$; and $\lim_{\left|m_{n_i}^{k-1}\right| \to \infty} W\left(m_{n_i}^{k-1}\right) = \infty$.

Thus, $W\left(m_{n_i}^k\right)$ are convex over K periods, which means the minimising scalars T_{n_i} exist. Thus, the proof of Theorem 1 is completed.

5.2. Optimal duty cycle control

According to the optimal transmission policy, by substituting the optimal value of $r_{n_i}^k$ into (16), the optimal duty cycle control for IEEE 802.15.4 is derived as

$$SO_{n_i}^{k*} = \begin{cases} \left\lceil \log_2\left(\frac{r_{n_i}^{k*} \times P_s}{b} + D_{bcn}\right) \right\rceil & \text{if } q_{n_i}(k) < T_{n_i}, \\ \lceil \log_2(D_{bcn}) \rceil & \text{if } q_{n_i}(k) \geqslant T_{n_i} \end{cases} \tag{32}$$

The optimal duty cycle control is a multi-period policy: for each period k, before the gateway or the coordinator n_i make the decision on the duty cycle, it will check the current queue length $q_{n_i}^k$ first. If the queue length $q_{n_i}^k$ is smaller than the threshold $T_{n_i}^k$ of the optimal transmission policy, the *SO* of current period is set based on the optimal number of packets it should receive, which is decided by transmission policy; otherwise, *SO* is set to its minimum value $\lceil \log_2(D_{bcn}) \rceil$, according to (16).

5.3. Optimal duty cycle control algorithms

In this section, two DP algorithms are proposed to compute the optimal duty cycle control.

The first algorithm is a standard dynamic programming approach to recursively compute the optimal solution in a backward fashion, named DP optimal control. First, the cost-to-go function $U\left(r_{n_i}^k\right)$ is computed from period K back to period 0. Then, the transmission policy from period 0 to period K are selected with the minimum $U\left(r_{n_i}^k\right)$, and the duty cycle control is decided based on the selected transmission policy. The specific algorithm is given in Algorithm 1.

As stated in Section 5.3, the optimal transmission policy has a threshold structure. The second algorithm is PI algorithm based duty cycle control (PI optimal control). The exact embodiment of the algorithm is given in Algorithm 2. Because of the limitation of the buffer size, the duty cycle control in this paper has finite action and state spaces as well as bounded and stationary immediate cost functions.

Trans. Emerging Tel. Tech. **26**:56–69 (2015) © 2014 John Wiley & Sons, Ltd.
DOI: 10.1002/ett

Algorithm 1 Dynamic programming duty cycle control

Require: number of device N, control period K

for each $n_i \in N$ **do**
  Initialise $r_{n_i}^0$ arbitrarily and $U\left(r_{n_i}^K\right) = 0$
  for $k = K-1 \rightarrow 0$ **do**
    for each $r_{n_i}^k \leqslant q_{n_i}^{max}$ **do**
      Calculate $J\left(r_{n_i}^k\right)$
    end for
    $U\left(r_{n_i}^k\right) \leftarrow \sum_{k=k}^{K} J\left(r_{n_i}^k\right) + U\left(r_{n_i}^{k+1}\right)$
  end for
  for $k = 0 \rightarrow K$ **do**
    Step 1: Compute transmission policy
    $r_{n_i}^k \leftarrow \arg\min U\left(r_{n_i}^k\right)$
    Step 2: Assign the duty cycle
    $SO_{n_i}^k \leftarrow \left\lceil \log_2\left(\frac{r_{n_i}^k \times P_s}{b} + D_{bcn}\right)\right\rceil$
  end for
end for

Algorithm 2 Policy iteration algorithm-based duty cycle control

Require: number of device N, control period K

Initialise π, the policy to be evaluated arbitrarily, and policy-stable $\leftarrow$ false
for each $n_i \in N$ **do**
  Step 1: Compute transmission policy
  a) Policy evaluation:
  for $k = 0 \rightarrow K$ **do**
    $r_{n_i}^k \leftarrow \pi$
    $U\left(r_{n_i}^k\right) \leftarrow \sum_{k=0}^{K} J\left(r_{n_i}^k\right) + U\left(r_{n_i}^{k+1}\right)$
  end for
  b) Policy improvement:
  for each $\pi \in \mathcal{D}$ **do**
    $r_{n_i}^k \leftarrow \arg\min U\left(r_{n_i}^k\right)$
    if $r_{n_i}^k = \pi$ **then**
      policy-stable $\leftarrow$ true
    end if
    if policy-stable = true **then**
      stop
    elsego to 2.
    end if
  end for
  Step 2: Assign the duty cycle
  for $k = 0 \rightarrow K$ **do**
    $r_{n_i}^{k+1} \leftarrow \pi$
    $SO_{n_i}^k \leftarrow \left\lceil \log_2\left(\frac{r_{n_i}^k \times P_s}{b} + D_{bcn}\right)\right\rceil$
  end for
end for

Under these conditions PI algorithm is proven to converge to the optimal policy [43].

Policy iteration optimal control is based on two steps: (i) policy evaluation and (ii) policy improvement. In the policy evaluation step, the value of a policy π is evaluated by computing the cost-to-go function $U_\pi\left(r_{n_i}^k\right)$. In the policy improvement step, the PI algorithm looks for a policy π' that is better than the previously evaluated policy π. Thus, the heuristic-based policies are applied accordingly in the policy improvement step to minimise the cost-to-go function $U\left(r_{n_i}^k\right)$. When the same policy is found in two consecutive iterations, we conclude that the algorithm has converged. The performance of the proposed algorithm and the comparison with other approaches will be given in Section 7.

6. SUBOPTIMAL DUTY CYCLE CONTROL

As the optimal solution is difficult or impractical to implement on computation-limited sensor devices, we further propose a low-complexity RADutyCon and also give its joint-cost upper bound.

Based on the aforementioned analysis, the optimal duty cycle of device n_i can be found by running DP algorithms. However, both Algorithms 1 and 2 need to conduct exhaustive search over possible solutions at each period, which is very energy inefficient and time consuming. Thus, it is difficult or impractical for computationally limited sensor devices to run DP.

Rollout algorithms have demonstrated excellent performance on a variety of dynamic optimisation problems. Interpreted as an approximate DP algorithm, a rollout algorithm estimates the cost-to-go at each period by estimating future costs whilst following a heuristic control, referred to as the base policy. The heuristic base control in this paper is inspired by the threshold structure of the optimal control. In order to ensure the stable of the queue length, the device should receive same number of packets as it transmits at each period. Thus, instead of searching the optimal solution by running DP, the most straightforward approach is to set T_{n_i} equals to the mean value of $f_{n_i}^k$ for each device n_i. Based on (18), the heuristic base control of $\mathcal{P}_{n_i}$ is given as

$$SO_{n_i}^k = \begin{cases} \left\lceil \log_2\left(\frac{r_{n_i}^k \times P_s}{b} + D_{bcn}\right)\right\rceil & \text{if } q_{n_i}(k) < f_{n_i}^k, \\ \lceil \log_2(D_{bcn}) \rceil & \text{if } q_{n_i}(k) \geqslant f_{n_i}^k \end{cases} \tag{33}$$

The proposed RADutyCon, as shown in Algorithm 3, is the one that attains the minimum of the cost-to-go function

$$U\left(r_{n_i}^k\right) = \min_{\pi_{n_i} \in \mathfrak{D}} \left[\mathbb{E}\left\{\alpha\left(E_r\left(r_{n_i}^k\right) + E_f\left(f_{n_i}^k\right) + E_l\left(r_{n_i}^k\right)\right) + \beta D\left(r_{n_i}^k\right) + \mathbb{E}\left\{\tilde{U}\left(r_{n_i}^{k+1}\right)\right\}\right\}\right] \tag{34}$$

where $\tilde{U}\left(r_{n_i}^{k+1}\right)$ is the approximation of $U\left(r_{n_i}^{k+1}\right)$ based on the heuristic base control.

Algorithm 3 Rollout algorithm base duty cycle control

Require: number of device N, control period K

for each $n_i \in N$ **do**
  for $k = 0 \rightarrow K$ **do**
    Step 1: Compute transmission policy
    a) Base policy estimation
    for $k = k + 1 \rightarrow K$ **do**
      $T_{n_i}^{k+1} \leftarrow f_{n_i}^{k+1}$
      if $q_{n_i}^{k+1} < T_{n_i}^{k+1}$ **then**
        $r_{n_i}^{k+1} \leftarrow T_{n_i}^{k+1} - q_{ni}^{k+1}$
      else
        $r_{n_i}^{k+1} \leftarrow 0$
      end if
      Calculate $J\left(r_{n_i}^{k+1}\right)$
    end for
    $\tilde{U}\left(r_{n_i}^{k+1}\right) \leftarrow \sum_{k=k+1}^{K} J\left(r_{n_i}^{k}\right)$
    b) Rollout algorithm based control
    for each $r_{n_i}^{k} \in \bar{\mathfrak{D}}$ **do**
      Calculate $J\left(r_{n_i}^{k}\right)$
      $U\left(r_{n_i}^{k}\right) \leftarrow J\left(r_{n_i}^{k}\right) + \tilde{U}\left(r_{n_i}^{k+1}\right)$
    end for
    $r_{n_i}^{k} \leftarrow \arg\min U\left(r_{n_i}^{k}\right)$
    Step 2: Assign the duty cycle
    $SO_{n_i}^{k} \leftarrow \left\lceil \log_2\left(\frac{r_{n_i}^{k} \times P_s}{b} + D_{bcn}\right)\right\rceil$
  end for
end for

Given the approximations $\tilde{U}\left(r_{n_i}^{k}\right)$, which is calculated based on the heuristic base control, the computational saving of RADutyCon is evident, as only a single minimisation problem has to be solved at each period. Noticed that even with readily available approximations $\tilde{U}\left(r_{n_i}^{k+1}\right)$, the calculation of the minimisation over $\pi_{n_i} \in \mathfrak{D}$ may involve substantial computation. To further save the computation, a subset $\bar{\mathfrak{D}}$ of the promising controls is identified in the proposed RADutyCon. Thus, the minimisation over $\mathfrak{D}$ in (20) is replaced by a minimisation over a subset $\bar{\mathfrak{D}} \subset \mathfrak{D}$.

Theorem 2. *Let us denote $\hat{U}\left(r_{n_i}^{k}\right)$ as the estimate cost-to-go of RADutyCon, whose control range is $\bar{\mathfrak{D}} \subset \mathfrak{D}$. $U\left(r_{n_i}^{k}\right)$ as the expected actual cost-to-go incurred by RADutyCon. Then, we have $U\left(r_{n_i}^{k}\right) \leqslant \tilde{U}\left(r_{n_i}^{k}\right)$, which means $\tilde{U}\left(r_{n_i}^{k}\right)$ is the cost-to-go upper bound of RADutyCon.*

Proof. For $k = 0, 1, \cdots, K-1$ denote

$$\hat{U}\left(r_{n_i}^{k}\right) = \min_{\pi_{n_i} \in \bar{\mathfrak{D}}} \left[\mathbb{E}\left\{\alpha\left(E_r\left(r_{n_i}^{k}\right) + E_f\left(f_{n_i}^{k}\right) + E_l\left(r_{n_i}^{k}\right)\right) + \beta D\left(r_{n_i}^{k}\right) + \mathbb{E}\left\{\tilde{U}\left(r_{n_i}^{k+1}\right)\right\}\right\}\right] \tag{35}$$

Thus for all $q_{n_i}^{k}$, we have $\hat{U}\left(r_{n_i}^{k}\right) \leqslant \tilde{U}\left(r_{n_i}^{k}\right)$, let

$$\begin{aligned}\hat{U}\left(r_{n_i}^{K}\right) &= G\left(r_{n_i}^{K}\right) \\ &= \alpha\left(E_r\left(r_{n_i}^{K}\right) + E_f\left(f_{n_i}^{K}\right) + E_l\left(r_{n_i}^{K}\right)\right) + \beta D\left(r_{n_i}^{K}\right)\end{aligned} \tag{36}$$

Applying backward induction on k, we have $U\left(r_{n_i}^{k}\right) = \hat{U}\left(r_{n_i}^{K}\right) = G\left(r_{n_i}^{K}\right)$ for all $q_{n_i}^{K}$. Assuming that $\bar{U}\left(r_{n_i}^{k+1}\right) \leqslant \hat{U}\left(r_{n_i}^{k+1}\right)$ for all $q_{n_i}^{k+1}$, we have

$$\begin{aligned}U\left(r_{n_i}^{k}\right) &= \mathbb{E}\left\{G\left(r_{n_i}^{k}\right) + \bar{U}\left(r_{n_i}^{k+1}\right)\right\} \\ &\leqslant \mathbb{E}\left\{G\left(r_{n_i}^{k}\right) + \hat{U}\left(r_{n_i}^{k+1}\right)\right\} \\ &\leqslant \mathbb{E}\left\{G\left(r_{n_i}^{k}\right) + \tilde{U}\left(r_{n_i}^{k+1}\right)\right\} = \hat{U}\left(r_{n_i}^{k}\right)\end{aligned} \tag{37}$$

for all $q_{n_i}^{k}$. The first equality in the succeeding text follows from the definition of the cost-to-go $U\left(r_{n_i}^{k}\right)$ of RADutyCon, whilst the first inequality follows from the induction hypothesis, and the second inequality follow from the assumption $\hat{U}\left(r_{n_i}^{k}\right) \leqslant \tilde{U}\left(r_{n_i}^{k}\right)$. Then, we have $U\left(r_{n_i}^{k}\right) \leqslant \hat{U}\left(r_{n_i}^{k}\right) \leqslant \tilde{U}\left(r_{n_i}^{k}\right)$ for all $q_{n_i}^{k}$. Thus, the $\tilde{U}\left(r_{n_i}^{k}\right)$ is a readily obtainable performance upper bound for the cost-to-go function $U\left(r_{n_i}^{k}\right)$.

In addition, two remarks of the proposed RADutyCon are given as follows.

Remark 1. The proposed RADutyCon has lower computation complexity as compared with the DP optimal control. If D is the average search range of the devices, the computation complexity of DP algorithm is $O(KD^{N+D})$, whilst that of the RADutyCon is only $O(KND)$.

Remark 2. The proposed suboptimal controls have lower synchronisation overhead as compared with controls in [35] and [36]. The proposed control does not need additional SYNC packet to ensure the devices are active at the same time as it employs the same *BO* as defined in IEEE 802.15.4 (2011), and all devices are activated at the beginning of each *BI*.

7. SIMULATION RESULTS AND ANALYSIS

In this section, we applied the DP and PI optimal controls on the gateway and the coordinator, respectively. The performance of the two optimal control algorithms is compared. Then, we evaluate the proposed RADutyCon in two scenarios, where RADutyCon is applied on coordinators of capillary networks and gateways, respectively.

The performance metrics are average energy efficiency, average end-to-end delay and average packet drop ratio. The average energy efficiency is calculated as the total amount of data over the total energy consumption of K periods, and the average end-to-end delay is the total buffered time of the packets over the total number of generated packets in the network. Packet drop ratio is calculated

Trans. Emerging Tel. Tech. **26**:56–69 (2015) © 2014 John Wiley & Sons, Ltd.
DOI: 10.1002/ett

Table I. Energy consumption and buffer parameters.

Device	Parameter	Value	Device	Parameter	Value
Coordinator	Buffer size	600 bytes	M2M gateway	Buffer size	1524 bytes
	Device sensitivity	−90 dBm		Device sensitivity	−110 dBm
	Transmit power	36.5 mw		Transmit power	20 w
	Receiving power	41.4 mw		Receiving power	3.0 w
	Idle listen power	41.4 mw		Idle listen power	3.0 w
	Sleep power	0.042 mw		Sleep power	0.05 w

Table II. Simulation parameters.

Parameter	Value
IEEE 802.15.4 data rate	250 kbps
LTE data rate	50 Mbps
CCA size	8 symbols
ACK packet size	10 symbols
Unit backoff period	20 symbols
Packet size	10 bytes

as the number of packets have been dropped because of the excess maximum queue length over the total number of the generated packets.

To make the simulation scenario more general, the M2M devices are Poisson random deployed in each realisation. The mean value of M2M devices number for each coordinator is 20, and the number of coordinator for each gateway is 2. Because devices switch between active and inactive modes, we applied ON/OFF traffic model in the simulation. When the device is active (ON), the data arrival rate follows a Poisson distribution. When the device is inactive (OFF), it is idle and does not generate any packets. Packets are dropped when the queue length of the device reaches its maximum $q_{n_i}^{\max}$.

Energy consumption parameters for gateways and coordinators are based on Cisco 819 [44] and Texas Instruments CC2420 [45], respectively. Specific energy parameters for gateways and coordinators are given in Table I.

The duration of each period (BI) is 0.49 s with $BO = 5$. The number of observation periods K is 100. MAC layer parameters are based on IEEE 802.15.4-2011 standard. We set α to 0.2 and β to 0.4. The results are the averaged values of 1000 runs, and other simulation parameters are given in Table II.

7.1. Optimal duty cycle control performance

In this part, we compare the performance of two optimal duty cycle controls. Due to the space limitation, we only show the result when the proposed scheme is applied on the coordinator, whilst the results trend of these two controls are very similar.

We omit the result figure of cost function value, as the averaged cost value difference between two optimal control algorithms is much less than 0.1%. From Figures 3 and 4, we can see that compared with the DP optimal control, the PI optimal control achieved 67.3% reduction of end-to-end delay with 43.9% sacrifice on energy efficiency on average.

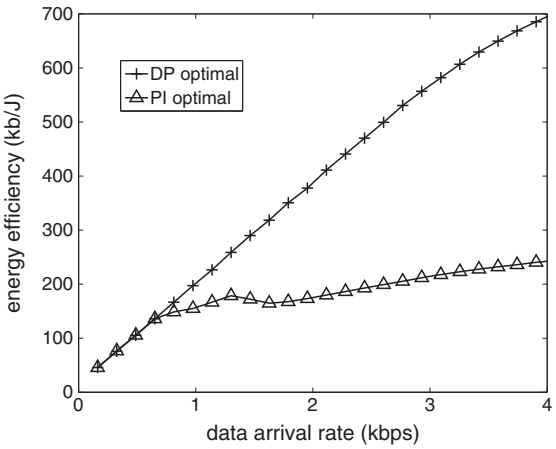

Figure 3. Energy efficiency of optimal duty cycle control.

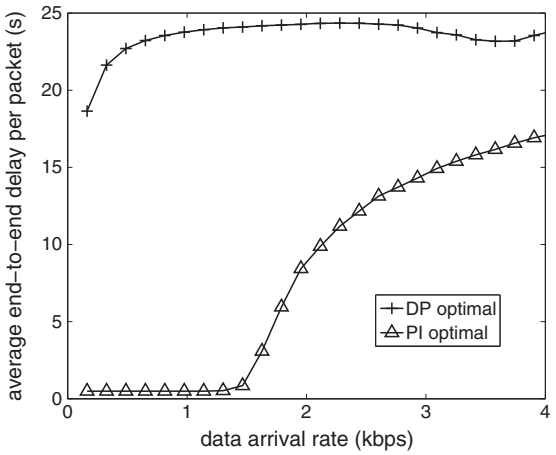

Figure 4. End-to-end delay of optimal duty cycle control.

The packet drop ratio in Figure 5 shows that no packet drop is observed when data arrival rate is less than 1 kbps for both DP optimal control and PI optimal control. The packet drop ratio of PI optimal control is slightly less than that of DP optimal control.

Because both coordinators and gateways are supposed to have sufficient power supply, with significant achievement of end-to-end delay reduction and negligible cost value

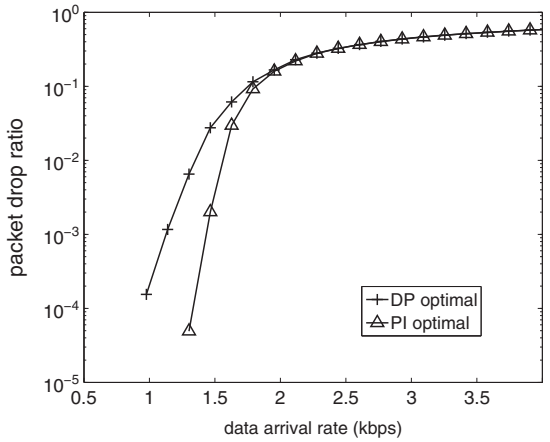

Figure 5. Packet drop ratio of optimal duty cycle control.

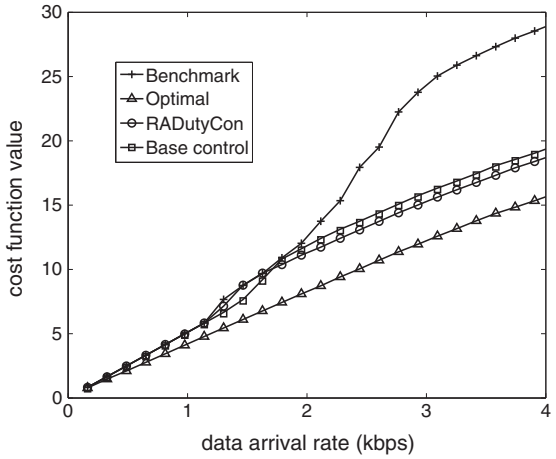

Figure 6. Cost function value of RADutyCon on coordinator.

difference, the PI optimal control outperforms the DP optimal control in our scenario. Thus, we applied PI optimal control to compute the optimal duty cycle control in the rest of our simulations.

7.2. Suboptimal RADutyCon performance

In this part, we apply the proposed RADutyCon on gateways and coordinators. The performance of the proposed RADutyCon is compared with that of a benchmark control, the optimal control, and the heuristic base control of RADutyCon.

Benchmark control: to reduce the end-to-end delay, the benchmark control aims at maximising the number of received packets $r_{n_i}^k$. The *SO* is determined based on (16), and the maximum *SO* is bounded by the service rate $f_{n_i}^k$ of the device.

Optimal control: Based on Theorem 1, the optimal $r_{n_i}^{k*}$ follows threshold structure. The optimal duty cycle control in this section is computed by PI-based control algorithm.

Base control: the heuristic base control has a fixed threshold equals to $f_{n_i}^k$. Thus, $r_{n_i}^k = f_{n_i}^k - q_{n_i}^k$, and the value of the *SO* is determined based on (27). The maximum *SO* is bounded by the predefined value $f_{n_i}^k$.

RADutyCon: RADutyCon will do one search at each period to find the minimum value of (20), whilst the future cost is estimated by applying the heuristic based control. The value of the optimal SO^* is determined based on (10), and the maximum *SO* is bounded the search range $\widetilde{\mathfrak{D}}$ at each period.

7.2.1. RADutyCon on coordinator.

It is shown in Figure 6 that the proposed RADutyCon has lower joint-cost as compared with the benchmark control and the base control by the average of 31% and 5.7%, respectively, over the range of evaluated traffic. The joint-cost of RADutyCon is slightly higher to that of the optimal control. Based on Theorem 2, the heuristic base control is the joint-cost upper bound for RADutyCon with different search ranges. The improvement of RADutyCon to the heuristic base control is achieved by searching the minimum of the cost-to-go function (20) at each period. According to Remark 1, RADutyCon will be more beneficial when coordinator n_i has large number of child devices with an exponential reduction of the computational complexity.

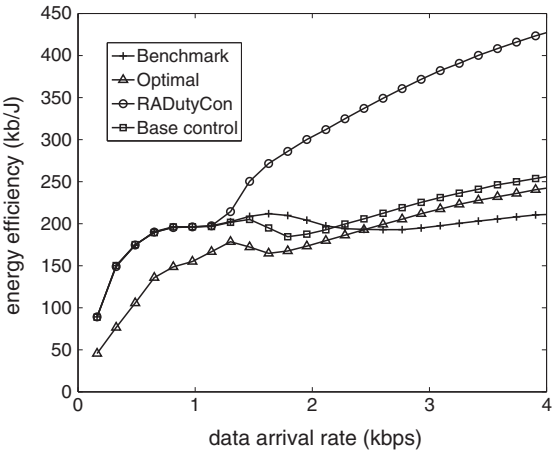

Figure 7. Energy efficiency of RADutyCon on coordinator.

Figure 7 shows the energy efficiency with different data arrival rates. The energy efficiency curves have a increase trend along with the increase of data arrival rates. The change of energy efficiency curve of RADutyCon between 0.8 and 1.5 kbps is because the radical increase of *SO*, which leads to higher idle listening energy consumption. The proposed RADutyCon achieves higher energy efficiency compared with benchmark control, the base control and the optimal control. After 30 packets/active period, the number of transmitted packets is relevant stable, thus the energy consumption curves keep flat for all examined controls.

Trans. Emerging Tel. Tech. **26**:56–69 (2015) © 2014 John Wiley & Sons, Ltd.
DOI: 10.1002/ett

The two-hop end-to-end delay from end devices to the M2M gateway of RADutyCon in Figure 8 is higher than that of the optimal control. The end-to-end delay of all evaluated control have increase trend with the increase of data arrival rates. Combined with Figure 7, it is clear that the increasing of energy efficiency is at the cost of increasing end-to-end delay.

Figure 9 shows the packet drop ratio of the evaluated controls. The packet drop ratio of RADutyCon has close performance compared with that of the heuristic base control and the optimal control. The packet drop ratio of RADutyCon is higher than that of the benchmark control because the reduced active periods of RADutyCon increases the number of buffered packets. Hence, the possibility of packet drop is increased due to limited maximum queue length.

7.2.2. RADutyCon on gateway.

Simulation results of RADutyCon running on gateways of the network are presented in this part. Since gateways have enough memory to buffer the packets, the packet drop ratio is zero in this scenario. The trend of simulation results in terms of cost function value, energy efficiency and end-to-end delay is similar to that when RADutyCon is applied on coordinators.

Compared Figure 10 with Figure 6, it is shown that when RADutyCon is applied on gateways, the cost value gap between RADutyCon and optimal control is higher than it is applied on coordinators. This is due to the reduced computation of RADutyCon. A linear increase of cost gap can be observed from Figure 10, whilst the computational complexity is reduced at expectational level.

The energy efficiency in Figure 11 are higher than that in Figure 7. This is because the gateways have larger memory storage than the coordinators. When the device is active, the larger buffer size ensure more available data to be transmitted, thus increase the energy efficiency.

When the data arrive rates are the same, the end-to-end delay in Figure 12 are much lower than that in Figure 8. This is because the gateway utilises high data rate LTE

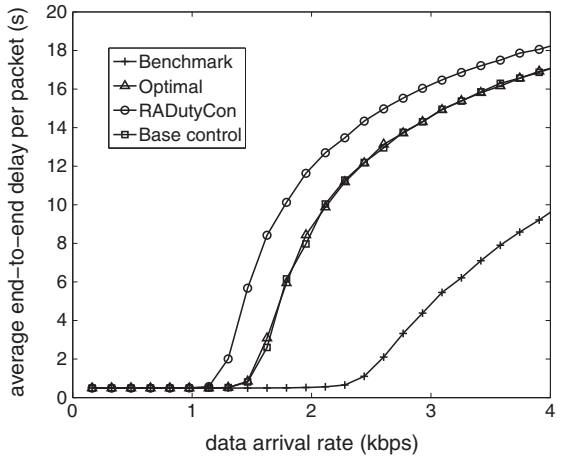

Figure 8. End-to-end delay of RADutyCon on coordinator.

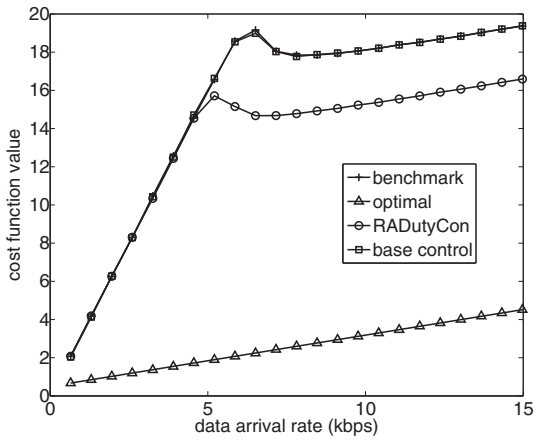

Figure 10. Cost of RADutyCon on gateway.

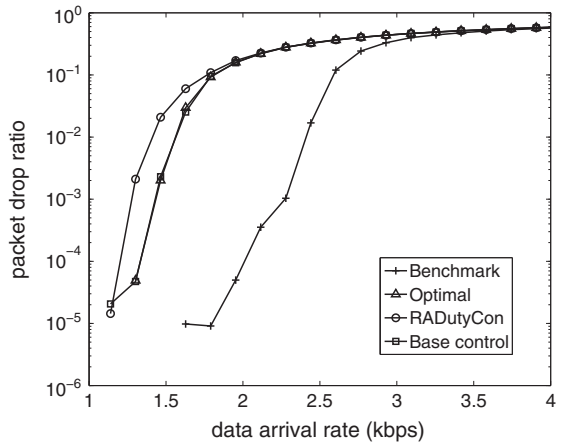

Figure 9. Packet drop ratio of RADutyCon on coordinator.

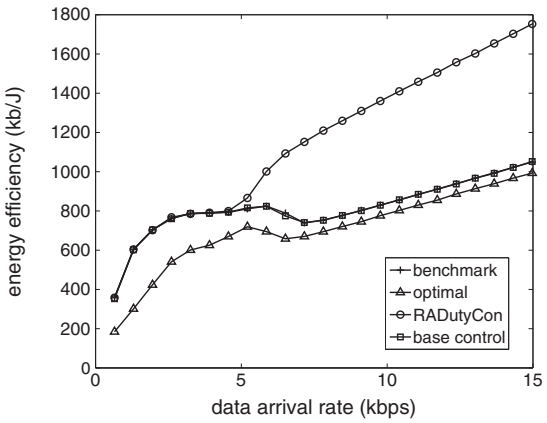

Figure 11. Energy efficiency of RADutyCon on gateway.

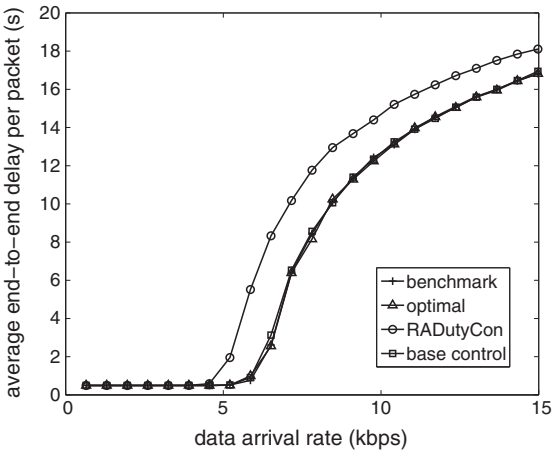

Figure 12. End-to-end delay of RADutyCon on gateway.

uplink transmission, whilst the coordinators utilises IEEE 802.15.4 low data rate link for uplink transmission.

8. CONCLUSION

To support the M2M communication in hybrid capillary networks and cellular networks, which are connected via gateways. In this paper, we proposed a distributed duty cycle control scheme, which is applicable on both the M2M gateway and the coordinator in capillary networks. The proposed duty cycle scheme aims at minimising the joint-cost of energy consumption and end-to-end delay. We analytically derived the optimal duty cycle control and proposed two algorithms to compute the optimal solution. Then RADutyCon is proposed to reduce the computation complexity. To evaluate the performance of the proposed RADutyCon, we applied RADutyCon on gateways, then coordinators. Simulation results show that for both the cases, RADutyCon can effectively reduce the joint-cost of energy consumption and end-to-end delay under various network traffic. RADutyCon achieved lower joint-costs over the benchmark control and the heuristic base control. The joint-cost is similar to that of optimal control. In addition, an exponential reduction of the computation complexity is achieved by RADutyCon.

REFERENCES

1. Chen J, Cao X, Cheng P, Xiao Y, Sun Y. Distributed collaborative control for industrial automation with wireless sensor and actuator networks. *IEEE Transactions on Industrial Electronics* 2010; **57**(12): 4219–4230.
2. Zhang Y, Yu R, Xie S, Yao W, Xiao Y, Guizani M. Home M2M networks: architecture, standards and QoS improvements. *IEEE Communications Magazine* 2011; **49**(4): 44–52.
3. Yu R, Zhang Y, Gjessing S, Xia W, Yang K. Toward cloud-based vehicular networks with efficient resource management. *IEEE Network Magazine* 2013; **27**(5): 48–55.
4. Cao X, Chen J, Zhang Y, Sun Y. Development of an integrated wireless sensor network micro-environmental monitoring system. *Elsevier ISA Transactions* 2008; **47**(3): 247–255.
5. Gau RH, Cheng CP. Optimal tree pruning for location update in machine-to-machine communications. *IEEE Transactions on Wireless Communications* 2013; **12**(6): 2620–2632.
6. Lien SY, Liau TH, Kao CY, Chen KC. Cooperative access class barring for machine-to-machine communications. *IEEE Transactions on Wireless Communications* 2012; **11**(1): 27–32.
7. Xia F, Yang LT, Wang L, Vinel A. Internet of things. *International Journal of Communication Systems* 2012; **25**(9): 1101–1102.
8. Gerasimenko M, Petrov V, Galinina O, Andreev S, Koucheryavy Y. Impact of machine-type communications on energy and delay performance of random access channel in LTE-advanced. *Transactions on Emerging Telecommunications Technologies* 2013; **24**: 366–377.
9. METIS. Initial report on horizontal topics, first results and 5G system concept, April 2014. Available from: https://www.metis2020.com/wp-content/uploads/deliverables/METISD6.2v1.pdf [Accessed on 1 October 2014].
10. 3GPP TS 22.368. Service requirements for machine-type communications (MTC), September 2011. v.11.3.0 (release 11).
11. 3GPP TR 23.888. System improvements for machine-type communications, November 2011. v.1.6.0 (release 11).
12. 3GPP TR 37.868. Study on RAN improvements for machine-type communications, September 2011. v.11.0.0 (release 11).
13. Yang B, Zhu G, Wu W, Gao Y. M2M access performance in LTE-A system. *Transactions on Emerging Telecommunications Technologies* 2014; **25**(1): 3–10.
14. Tirronen T, Larmo A, Sachs J, Lindoff B, Wiberg N. Machine-to-machine communication with long-term evolution with reduced device energy consumption. *Transactions on Emerging Telecommunications Technologies* 2013; **24**(4): 413–426.
15. Chin WH, Fan Z, Haines R. Emerging technologies and research challenges for 5G wireless networks. *IEEE Wireless Communications* 2014; **21**(2): 106–112.
16. Boccardi F, Heath RW, Lozano A, Marzetta TL, Popovski P. Five disruptive technology directions for 5G. *IEEE Communications Magazine* 2014; **52**(2): 74–80.
17. Wang C, Haider F, Gao X, *et al.* Cellular architecture and key technologies for 5G wireless communication net-

Trans. Emerging Tel. Tech. **26**:56–69 (2015) © 2014 John Wiley & Sons, Ltd.
DOI: 10.1002/ett

works. *IEEE Communications Magazine* 2014; **52** (2): 122–130.
18. Gotsis AG, Lioumpas AS, Alexiou A. Analytical modelling and performance evaluation of realistic time-controlled M2M scheduling over LTE cellular networks. *Transactions on Emerging Telecommunications Technologies* 2013; **24**(4): 378–388.
19. ETSI TS 102 690. *Machine-to-Machine communications (M2M): functional architecture,* Std. v.1.1.1, November 2011.
20. Zheng K, Hu F, Wang W, Xiang W, Dohler M. Radio resource allocation in LTE-advanced cellular networks with M2M communications. *IEEE Communications Magazine* 2012; **50**(7): 184–192.
21. Gotsis AG, Lioumpas AS, Alexiou A. M2M scheduling over LTE: challenges and new perspectives. *IEEE Vehicular Technology Magazine* 2012; **7** (3): 34–39.
22. Azimi V. Accommodating machine-to-machine traffic in IEEE 802.15.4: the prioritized wait time approach. *Theses and dissertations*, Department of Electrical and Computer Engineering, Ryerson University, Toronto, Ontario, Canada, 2012.
23. Project EXALTED. Available from: http://www.ict-exalted.eu [Accessed on 2 June 2014].
24. Cisco project. Available from: http://www.fiercewireless.com/tech/story/cisco-introduces-small-m2m-gateway-businesses/2011-08-25 [2 June 2014].
25. AnyBridge project. Available from: http://www.anybridge-m2m.nl/home [2 June 2014].
26. Systech project. Available from: http://www.systech.com [2 June 2014].
27. Alcatel-Lucent project. Available from: http://www2.alcatel-lucent.com/techzine/expanding-the-mobile-service-providers-role-in-m2m/ [2 June 2014].
28. M2M technology: challenge and opportunities. Available from: http://www.techmahindra.com/pages/default.aspx [2 June 2014].
29. IoT-A Project. Available from: http://www.iot-a.eu [2 June 2014].
30. IEEE std. 802.15.4. Part. 15.4: wireless medium access control (MAC) and physical layer (PHY) Specifications for Low-Rate Wireless Personal Area Networks (LR-WPANs), 2011. IEEE Std.
31. Misic J, Misic VB. *Wireless Personal Area Networks; Performance, Interconnections, and Security with IEEE 802.15.4*. John Wiley and Sons: Chichester, UK, 2008.
32. Xia F, Vinel A, Gao R, Wang L, Qiu T. Evaluating IEEE 802.15. 4 for cyber-physical systems. *EURASIP Journal on Wireless Communications and Networking*; **2011**: Article ID 596397, 14 pages.
33. Zhang L, Ferrero R, Sanchez ER, Rebaudengo M. Performance analysis of reliable flooding in duty-cycle wireless sensor networks. *Transactions on Emerging Telecommunications Technologies* 2014; **25**(2): 183–198.
34. Palattella MR, Accettura N, Dohler M, Grieco LA, Boggia G. Traffic aware scheduling algorithm for reliable low-power multi- hop IEEE 802.15.4e networks. In *Proceedings of IEEE International Symposium on Personal, Indoor and Mobile Radio Communications, PIMRC*, 2012.
35. Wang X, Wang X, Xing G, Yao Y. Dynamic duty cycle control for end-to-end delay guarantees in wireless sensor networks. In *Proceedings of IEEE International Workshop on Quality of Service, IWQoS*, Beijing, China, 2010.
36. Byun H, Yu J. Adaptive duty cycle control with queue management in wireless sensor networks. *IEEE Transactions on Mobile Computing* 2013; **12**(6): 1214–1224.
37. Park P, Ergen SC, Fischione C, Vincentelli AS. Duty-cycle oprimization for IEEE 802.15.4 wireless sensor networks. *ACM Transactions on Sensor Networks* 2013; **10**(1): 12:1–12:32.
38. Li Y, Chai KK, Chen Y, Loo J. Low complexity duty cycle control with joint-optimazation of delay and energy efficiency for beacon-enabled IEEE 802.15.4 networks. In *Proceedings of the 20th European Wireless, EW'14*, 2014.
39. 3GPP R1-120056. Analysis on traffic model and characteristics for MTC and text proposal, TSG-RAN Meeting WG1#68, *Technical Report*, Dresden, Germany, February 2012.
40. NIST.NIST priority action plan 2 guidelines for assessing wireless standards for smart grid. Applications.
41. Park TR, Kim TH, Choi JY, Choi S, Kwon WH. Throughput and energy consumption analysis of IEEE 802.15.4 slotted CSMA/CA. *Electronics Letters* 2005; **41**(18): 1017–1019.
42. Bertsekas DP. *Dynamic Programming and Optimal Control* (3rd edn). Athena Scientific: Belmont, Massachusetts, 2005.
43. John NT. On the Convergence of Optimistic Policy Iteration. *Journal of Machine Learning Research* 2002; **3**: 59–72.
44. Cisco 819 Machine to Machine Integrated Services Routers. Available from: http://www.cisco.com/c/en/us/products/collateral/routers/819-integrated-services-router-isr/datasheetc78-678459.html [2 June 2014].
45. CC2420 2.4 GHz IEEE 802.15.4 Compliant and ZigBee Ready RF Transceiver. Available from: http://www.ti.com/product/cc2420 [2 June 2014].